Deterministic Loading of Individual Atoms to a High-Finesse Optical Cavity

Kevin M. Fortier, Soo Y. Kim, Michael J. Gibbons, Peyman Ahmadi, and Michael S. Chapman

School of Physics, Georgia Institute of Technology, Atlanta, Georgia 30332-0430, USA

(Received 16 March 2007; published 8 June 2007)

Individual laser-cooled atoms are delivered on demand from a single atom magneto-optic trap to a high-finesse optical cavity using an atom conveyor. Strong coupling of the atom with the cavity field allows simultaneous cooling and detection of individual atoms for time scales exceeding 15 s. The single atom scatter rate is studied as a function of probe-cavity detuning and probe Rabi frequency, and the experimental results are in qualitative agreement with theoretical predictions. We demonstrate the ability to manipulate the position of a single atom relative to the cavity mode with excellent control and reproducibility.

DOI: 10.1103/PhysRevLett.98.233601 PACS numbers: 42.50.Pq, 32.80.Pj, 42.50.Vk

Cavity QED systems consisting of individual atoms localized in high-finesse optical micro-cavities are a fundamental system in quantum optics and have important applications to quantum information processing [1,2]. The intrinsic entanglement of atoms within the cavity mode and the cavity field provides a means to reversibly transfer quantum information between matter and light, and the eventual leakage of a photon from the well-defined mode of the cavity provides a means for high-fidelity, long-distance quantum communication. Although there has been recent progress in generating probabilistic atom-photon entanglements using free-space coupling of individual atoms [3,4] and collective excitations of atomic ensembles [5–7], only cavity QED systems in the strong coupling regime can provide both high entanglement probability and individual atomic qubits that can be independently manipulated.

The unique capabilities of optical cavity QED systems require controllably localizing individual atoms inside high-finesse, sub-mm length optical cavities. In the last decade, there has been considerable progress in integrating laser-cooled and trapped atoms with optical cavity QED systems in the strong coupling regime [8–18]. Individual atoms have been cooled and stored in optical cavities for time spans exceeding a second [10,18], and these advances have allowed demonstration of single photon sources and studies of the cavity QED system [13,14,17].

Previous experimental efforts have relied on probabilistic loading of laser-cooled atoms into the cavity from free-falling atoms or from an unknown number of atoms transferred from optical dipole traps [10,15]. Eventually, practical applications will require deterministic loading methods of single atoms into the cavity. In this Letter, we realize this goal by incorporating a deterministically loaded atom conveyor [19] that is used to deliver a precise number of atoms into a high-finesse resonator. We achieve storage times exceeding 15 s for atoms in the cavity with continuous cooling and observation using cavity-assisted cooling [10,20]. The atom-cavity interaction is studied as a function of probe-cavity detuning and probe Rabi frequency, and the experimental results are in good agreement with theoretical predictions. We demonstrate the ability to manipulate the position of a single atom relative to the cavity mode with excellent control and reproducibility. The use of an atom conveyor was suggested in [21] as a means to scale cavity QED interactions to many atomic qubits, and the results of this work represent an important step towards this goal.

A schematic of the experiment is illustrated in Fig. 1. A magneto-optical trap (MOT) of ^{87}Rb atoms is formed 8.5 mm away from a high-finesse optical cavity. The atoms are counted in the MOT with single atom resolution. Then they are transported from the MOT to the cavity using an atom conveyor [19] consisting of a 1D optical lattice formed by two independent counterpropagating laser beams from a fiber laser operating at $\lambda = 1064$ nm. The frequency of each lattice beam is controlled by an acousto-optic modulator (AOM) and by introducing a frequency difference between the counter-propagating beams, the trapped atoms can be transported to the cavity. This lattice is focused at the cavity with a waist, $w_0 = 34$ μm and provides a trapping potential of $U/k_B = 1$ mK with 4 W optical power per beam. The potential depth is only 100 μK at the MOT location (8.5 mm away) due to beam divergence. To increase the loading probability of a single atom from the MOT into this shallow trap, a separate

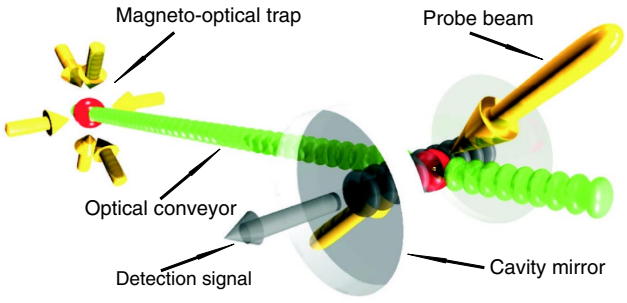

FIG. 1 (color online). A single atom MOT is formed 8.5 mm away from the optical cavity. The atom is loaded into an atom conveyor and then transported to the cavity mode. Inside the cavity, the atom is cooled via cavity-assisted cooling driven by counterpropagating probe beams.

loading lattice is employed. The loading lattice is orthogonal to the conveyor axis and formed from a retroreflected beam focused to a 17 μm waist at the MOT. For a loading lattice depth of 1 mK, realized with 1 W of laser power, we achieve 90% efficiency in transferring atoms from the MOT to the optical lattice.

The cavity is constructed from two superpolished concave mirrors ($r = 2.5$ cm) separated by 222 μm with total measured losses of 130 ppm. The relevant cavity QED parameters for this system are $(g_0, \kappa, \gamma/2) = 2\pi \times (17, 7, 3)$ MHz, where g_0, κ, and γ, are the maximum atom-cavity coupling rate, the cavity linewidth, and the natural linewidth of the $D2$ line ($5S_{1/2} \rightarrow 5P_{3/2}$) in ^{87}Rb, respectively. The single atom cooperativity is 13.7, putting the system in the strong coupling regime. The cavity length is actively stabilized to the $F = 2 \rightarrow F' = 3$ transition of the ^{87}Rb D2 line ($\lambda = 780$ nm) using an additional laser ($\lambda = 784$ nm) that is tuned to resonance with a different longitudinal mode of the cavity.

The experiment begins by collecting and counting individual atoms in the MOT. To load single or small numbers of atoms, the MOT is operated with magnetic field gradients of 250 G/cm to decrease the loading volume. This also provides tight confinement of the atoms, localizing the trapped atoms to an area of approximately 25×25 μm^2. The atoms are detected and counted by measuring the fluorescence of the atoms from the MOT cooling beams. This light is collected by a microscope objective (numerical aperture of 0.4) and focused onto an EMCCD (Andor IXon) camera. In Fig. 2, a typical time sequence of the MOT fluorescence is shown. The discrete jumps of the observed fluorescence signal correspond to individual atoms loading into or leaving the MOT. The losses due to background gas collisions are sufficiently rare to allow individual atoms to be trapped for more than 100 s. By

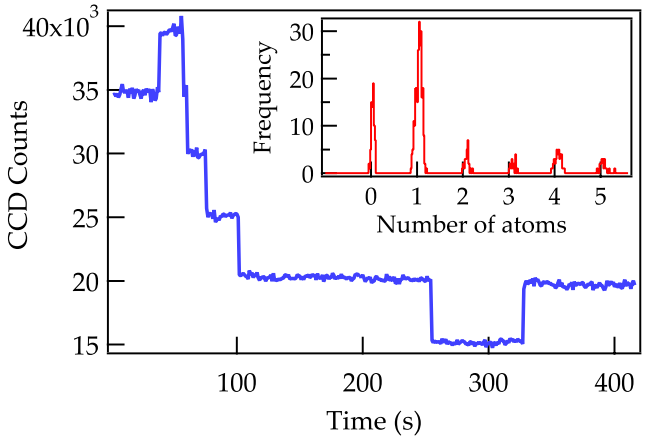

FIG. 2 (color online). The fluorescence signal collected from the high-gradient MOT with an exposure time of 500 ms per data point. Discrete steps indicate individual atoms captured or lost from the MOT. The inset shows a histogram of the integrated fluorescence signal of 0—5 trapped atoms.

exploiting the high quantum efficiency and the low noise of the camera and by carefully minimizing background light (principally stray scatter from the MOT beams), a single atom signal-to-noise ratio of $>$10:1 is achieved with a 500 ms integration time.

Once the atoms are loaded into the MOT and counted, they are loaded into the loading lattice. This is accomplished by turning on both the loading lattice and the conveyor lattice and, after a delay of 100 ms, turning off the MOT beams and magnetic field gradient. The atom(s) are then transferred to the conveyor lattice by ramping the loading lattice off in 75 ms. The atoms are transported to the cavity at a velocity of 2.6 cm/s by inducing a frequency difference of 50 kHz between the two counterpropagating beams of the conveyor lattice. The atoms are brought to rest inside the cavity mode by ramping the frequency difference to zero. The positioning reproducibility is estimated to be $<$10 μm, which corresponds to a relative position precision of 10^{-3}. The overall efficiency of transferring a known number of atoms counted in the MOT to the cavity is 80% for optimal conditions.

Once the atom is inside the mode of the high-finesse optical cavity, it is continuously detected and cooled using cavity-assisted cooling [10,22,23]. The atoms are excited by two counterpropagating probe beams, and radiation scattered from the atoms is reemitted into the cavity mode and subsequently detected by a photon counter as it leaks out the cavity. For positive cavity detunings with respect to the probe beams (i.e., $\Delta_C = \omega_c - \omega_p > 0$, where $\omega_{c,p}$ are the frequency of the cavity and the probe, respectively) the photon absorbed by the atom from the probe has lower energy than that emitted into the cavity mode, resulting in net cooling of the atom.

The probe beams are oriented 45° from the conveyor axis and have a lin $\perp$ lin polarization configuration. They are tuned 21.5 MHz below the $F = 2 \rightarrow F' = 3$ transition with a Rabi frequency of $\Omega = (2\pi)12$ MHz per beam and hence also provide conventional Doppler cooling along the probe beam direction. A hyperfine repumping laser beam copropagates with these beams to drive the $F = 1 \rightarrow F' = 2$ transition. The emitted photons from the cavity are detected with a single photon avalanche photodiode (APD).

Typical cavity emission signals corresponding to deterministically loaded atoms are shown in Figs. 3(a)–3(d) for different numbers of atoms initially loaded in the MOT ($N_{\text{atoms}} = 1$–4, respectively). In each case, the probe is turned on 250 ms after the atom(s) are brought to rest inside the cavity. The cavity emission signal is proportional to the number of atoms, and corresponds to a detected count rate of 10 counts/ms/atom. The particular data shown in Figs. 3(a)–3(d) show atom storage up to 4 s; however, the lifetime of the continuously cooled atoms in the cavity varies significantly depending on the exact experimental conditions and the number of atoms in the cavity. In general, for $N_{\text{atoms}} > 3$, the storage time is $<$1 s

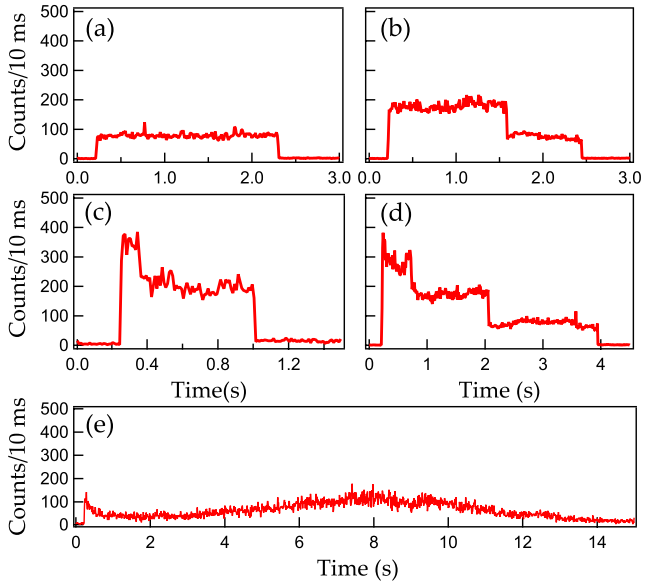

FIG. 3 (color online). Detected cavity emission signal vs time. In (a)–(d), the cavity emission signal corresponds to 1–4 atoms, respectively, initially loaded into the MOT and subsequently stored and detected in the cavity. In (e), storage of a single atom in the cavity for 15 s is shown.

for the experimental regime explored to date, while for $N_{\text{atoms}} = 1$–3, storage times of >15 s have been observed.

For optimal experimental conditions, we have observed single atom storage times exceeding 15 s with good reproducibility. A typical example of such a signal is shown in Fig. 3(e). The drift in the single atom count rate in this trace is due to a drifting frequency offset between the rf synthesizers that drive the conveyor AOMs. This results in a drift speed, $v \sim 0.5\ \mu$m/s, which eventually moves the atom out of the cavity mode.

According to the theoretical model of cavity-assisted cooling developed in [10,20], the rate at which a single atom scatters a photon into the cavity mode is given by

$$R = 2\kappa \frac{g^2}{\Delta_c^2 + \kappa^2} \frac{\Omega^2}{\Delta_a^2 + \gamma^2}, \qquad (1)$$

where $\Delta_a = \omega_0 - \omega_p + \Delta_S$ is the detuning of probe beam with respect to the atom resonance, ω_0, including the Stark shift, $\Delta_S \sim (2\pi)83$ MHz due to the conveyor optical lattice. For the experimental parameters of our system, Eq. (1) predicts an emission rate of $R = 2400$ photons/ms. Our detection efficiency is estimated to be 12.5%, including 50% quantum efficiency of the APD, 50% in propagation losses from the cavity to the APD and 50% loss due to detection only one of the possible polarizations of the light emitted by the cavity. Accounting for this detection efficiency, the predicted signal is 300 counts/ms, which is a factor of ~30 larger than measured in Fig. 3. This discrepancy varies from day-to-day; for optimal conditions, single atom signals as high as 30 counts/ms [10 times smaller than predicted by Eq. (1)] have been observed. Possible sources of signal discrepancy are nontransmission losses in the cavity mirrors and a reduced effective coupling due to the Zeeman structure of the atoms, and/or varying Stark shifts that depends on the alignment of the conveyor lattice.

One of the advantages of the use of external fields to trap the atom inside the cavity is that it allows control of the atom coupling via the position dependence of the atom-cavity interaction strength. In Fig. 4, this control is exploited both to investigate the position dependence of the coupling strength as well as to repeatably move an atom in and out of the cavity mode. For a Fabry-Perot cavity, the coherent coupling rate of the TEM_{00} Gaussian mode is given by $g(\mathbf{r}) = g_0 \cos(kz) \exp[-\rho^2/w^2]$ [1], written in a cylindrical coordinate system with z along the cavity axis and where w is the waist of the mode. To study the dependence of the coupling on the transverse coordinate, ρ, single atoms are slowly moved through the cavity mode (with a speed of 55 μm/s) while being continuously cooled and detected. The single atom signal vs position are shown in Fig. 4(a). The data, which are an average of 17 single atom runs, are fit well by a Gaussian function as expected from Eq. (1), however, the measured waist ($w_0 = 16\ \mu$m), is 20% smaller than the waist calculated from the cavity geometry (20 μm). The source of this discrepancy is not known, but could be related to the inadequacies of the two-level model assumed in Eq. (1) or involve subtle

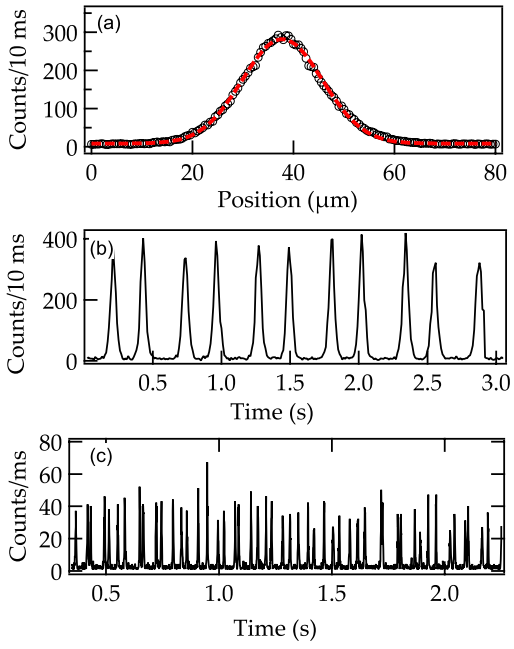

FIG. 4 (color online). In (a) an atom is swept across the cavity mode at a slow speed, $v = 55\ \mu$m/s, to achieve the high resolution scan shown. These data are the average of 17 experimental runs which are fit to a Gaussian function. (b) and (c) show a single atom swept across the cavity mode 10 and 75 times with a speed of 440 μm/s and 4.4 mm/s, respectively.

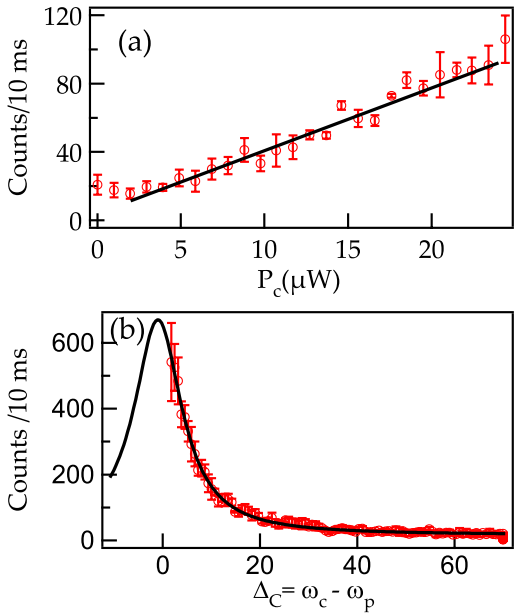

FIG. 5 (color online). (a) Single atom scattering rate versus probe beam power. The solid line is a linear fit to the data as expected from the dependence of the scattering rate to the probe beam power. The first three points are dark counts and are not included in the fit. (b) The dependence of the single atom scattering rate with respect to the cavity detuning Δ_C. The solid line is a fit to a Lorentzian function.

interplays between the cooling rate and the atom localization.

The atom conveyor allows for controllable and reversible introduction of the atom into the cavity mode. This is demonstrated in Fig. 4(b), which shows a single atom being moved in and out of the cavity 10 times. For this scan, the atomic speed was 440 μm/s. Moving at faster velocities, we have observed over 70 passes of a single atom across the cavity mode. Typical data for the faster scans are shown in Fig. 4(c).

We have measured the single atom signal as a function of the power of the probe beams and the detuning of the cavity as shown in Fig. 5. For the data in Fig. 5(a), the power in the probe beams is linearly ramped from 24 nW to 24 μW in 250 ms after a single atom has been loaded into the cavity. This corresponds to a variation in the Rabi frequency of $\Omega = (2\pi)0.8$–25 MHz. For these data the cavity detuning was -12 MHz and as expected from Eq. (1), the single atom signal is proportional to the power of the cooling beams ($\propto \Omega^2$). For the data in Fig. 5(b), a single atom is loaded in the cavity, and the probe-cavity detuning, $\Delta_C = \omega_c - \omega_p$, is varied by detuning the cavity while holding the frequency of the probe beam constant at $\omega_p = \omega_0 - 21.5$ MHz. Over the range of Δ_C that is investigated, the scattering rate shows a Lorentzian dependence on Δ_C, with a line center and linewidth of zero MHz and 6 MHz (HWHM) in close agreement with the measured cavity linewidth. This technique can only be used for investigating positive values of Δ_C because the negative values of Δ_C result in heating rather than cooling of the atoms [20] and lead to rapid loss of the trapped atoms. In conclusion, we have demonstrated the deterministic delivery of single atoms on demand to a high-finesse optical cavity. This was accomplished by loading single atoms from a high-gradient MOT into an atom conveyor and subsequently transporting them into an optical cavity. Employing cavity-assisted cooling, long storage times are observed. We also investigated the position dependence of the single atom scattering rate and the dependence of this rate on the power of the cooling beams and the detuning of the cavity. The results are in qualitative agreement with existing theoretical calculations.

The successful integration of an atom conveyor with a high-finesse cavity opens the door to a scalable cavity QED based quantum information processing system. Our next step towards this goal will be to create and manipulate qubit states within the atoms and to transfer these coherences to the optical cavity field. This will enable a diverse set of atom-photon entanglement protocols for quantum communications. Scaling the cavity-atom conveyor system to many tens of atoms is straightforward to envisage, although entangling large numbers atoms will require long coherence times of the atomic qubit states.

We would like to thank Paul Griffin for stimulating discussions. This work was supported by the NSF Grant No. PHY-0326315.

[1] P. R. Berman, *Cavity Quantum Electrodynamics* (Academic, San Diego, 1994).
[2] H. Mabuchi and A. C. Doherty, Science **298**, 1372 (2002).
[3] B. B. Blinov *et al.*, Nature (London) **428**, 153 (2004).
[4] J. Volz *et al.*, Phys. Rev. Lett. **96**, 030404 (2006).
[5] D. N. Matsukevich and A. Kuzmich, Science **306**, 663 (2004).
[6] D. N. Matsukevich *et al.*, Phys. Rev. Lett. **95**, 040405 (2005).
[7] C. W. Chou *et al.*, Nature (London) **438**, 828 (2005).
[8] A. D. Boozer *et al.*, Phys. Rev. Lett. **97**, 083602 (2006).
[9] S. Nußmann *et al.*, Phys. Rev. Lett. **95**, 173602 (2005).
[10] S. Nußmann *et al.*, Nature Phys. **1**, 122 (2005).
[11] P. Maunz *et al.*, Nature (London) **428**, 50 (2004).
[12] J. McKeever *et al.*, Phys. Rev. Lett. **93**, 143601 (2004).
[13] J. McKeever *et al.*, Science **303**, 1992 (2004).
[14] T. Legero *et al.*, Phys. Rev. Lett. **93**, 070503 (2004).
[15] J. A. Sauer *et al.*, Phys. Rev. A **69**, 051804(R) (2004).
[16] J. McKeever *et al.*, Phys. Rev. Lett. **90**, 133602 (2003).
[17] A. Kuhn *et al.*, Phys. Rev. Lett. **89**, 067901 (2002).
[18] J. Ye *et al.*, Phys. Rev. Lett. **83**, 4987 (1999).
[19] S. Kuhr *et al.*, Science **293**, 278 (2001).
[20] K. Murr *et al.*, Phys. Rev. A **73**, 063415 (2006).
[21] M. Barrett *et al.*, Bull. Am. Phys. Soc. **13**, 6 (1999).
[22] V. Vuletić and S. Chu, Phys. Rev. Lett. **84**, 3787 (2000).
[23] Hilton W. Chan *et al.*, Phys. Rev. Lett. **90**, 063003 (2003).